ISSN 1070-3284, Russian Journal of Coordination Chemistry, 2024, Vol. 50, No. 4, pp. 257–268. © Pleiades Publishing, Ltd., 2024.

Photoluminescent Lanthanide(III) Complexes Based on 2-[((4-Chlorophenyl)amino)methylene]-5,5-dimethylcyclohexane-1,3-dione

K. S. Smirnova[a], E. A. Sanzhenakova[a], I. V. El'tsov[b], I. P. Pozdnyakov[c], A. A. Russkikh[d], V. V. Dotsenko[d], and E. V. Lider[a, *]

[a] *Nikolaev Institute of Inorganic Chemistry, Siberian Branch, Russian Academy of Sciences, Novosibirsk, Russia*

[b] *Novosibirsk National Research State University, Novosibirsk, Russia*

[c] *Voevodskii Institute of Chemical Kinetics and Consumption, Siberian Branch, Russian Academy of Sciences, Novosibirsk, Russia*

[d] *Kuban State University, Krasnodar, Russia*

**e-mail: lisalider@gmail.com*

Received November 3, 2023; revised November 7, 2023; accepted November 7, 2023

Abstract—Five coordination compounds of the general formula $[LnL_2(NO_3)_3]_n$ (Ln^{3+} = Eu (**I**), Sm (**II**), Tb (**III**), Dy (**IV**), and Gd (**V**)) based on 2-[((4-chlorophenyl)amino)methylene]-5,5-dimethylcyclohexane-1,3-dione (L) are synthesized. The crystal structures of the ligand and complex **III** are determined by X-ray diffraction (XRD) analysis of single crystals (CIF files CCDC no. 2298715 (L) and 2298716 (**III**)). Complex **III** is polymeric due to the bidentate-bridging coordination of the ligand by the oxygen atoms of the cyclohexanedione fragment, and the coordination number of the central atom is ten. According to the powder XRD data, all synthesized polycrystalline compounds are isostructural to the single crystals of complex **III**. The photoluminescence properties of the ligand and coordination compounds in the polycrystalline state are studied. The energy transfer from the ligand to lanthanide(III) ion is shown to proceed via the "antenna" mechanism in the case of the europium(III), samarium(III), and terbium(III) compounds. Among the series of the complexes, the highest quantum yield is observed for compound **I** (21.9%), and the sensitization efficiency of the europium(III) complex is 43.5%.

Keywords: lanthanide(III) complexes, β-enaminedione, polymeric compounds, crystal structure, photoluminescence

DOI: 10.1134/S1070328423601450

INTRODUCTION

Coordination chemistry of rare-earth elements (REE) is an actively developed trend in chemistry [1–10]. These compounds attract attention due to their luminescence properties: each element is characterized by the emission range, and the total luminescence of the lanthanide(III) complexes appears from the near-UV to IR ranges of electromagnetic radiation. The REE coordination compounds mainly emit via the "antenna" mechanism based on the energy transfer from the ligand to lanthanide(III) ion [11]. Various oxygen-, nitrogen-, phosphorus-, and sulfur-containing organic compounds act as ligands, and the list of possible ligands for the synthesis of REE complexes with high luminescence characteristics continues to extend. Enaminones exemplify the "new" poorly studied ligands being compounds with the nonaromatic unit $R_2N–C(H)=C(H)–C(H)=O$, where the carbonyl and enamine $R_2N–C(H)=CH_2$ fragments form a conjugated system assuming the formation of an intramolecular hydrogen bond. These compounds are universal precursors for organic synthesis [12–21] and have such attractive properties as biological activity [22–27] and fluorescence [28, 29].

2-[((4-Chlorophenyl)amino)methylene]-5,5-dimethylcyclohexane-1,3-dione (L) was used as the ligand. The lanthanide(III) complexes based on 2-[((phenyl)-amino)methylene]-5,5-dimethylcyclohexane-1,3-dione and its *para*- and *meta*-methoxysubstituted derivatives have previously been synthesized and structurally characterized [30–32]. The ligand without substituents in the benzene ring was found to exhibit both the monodentate and bidentate-bridging coordination modes, which results in the formation of the polymeric chain complexes [30]. The REE complexes with the methoxysubstituted derivatives are polymeric layered compounds due to the bidentate-bridging coordination of the ligands. Among these ligands, the maximum quantum yield is achieved for the *para*-methoxy derivative (41%), whereas that of the europium(III) compound with the unsubstituted derivative is highest among the complexes (15%).

The synthesis of ligand L has previously been described in a number of works. For instance, the reaction of 4-chlorophenylisonitrile with dimedone in the presence of di(*tert*-butyl) peroxide in dichloroethane at 80°C afforded compound L in a yield of 84% [33]. Enaminodiketone can be synthesized in a yield of 65% by the reaction of 5,5-dimethyl-2-(ethoxymethylene)cyclohexane-1,3-dione with 4-chloroaniline on reflux in 1,4-dioxane [34]. In addition, the ligand can be isolated in high yields upon the short-term heating (120–130°C) of a mixture of triethyl orthoformate, 4-chloroaniline, and dimedone [35–39] (Scheme 1). Similar 2-(anilinomethylene)-1,3-diketones themselves are of interest as herbicides [37], potential antitubercular agents [36], functional building blocks for fine organic synthesis [40–46], and promising ligands for the preparation of coordination compounds of transition metals [30–32, 47–49].

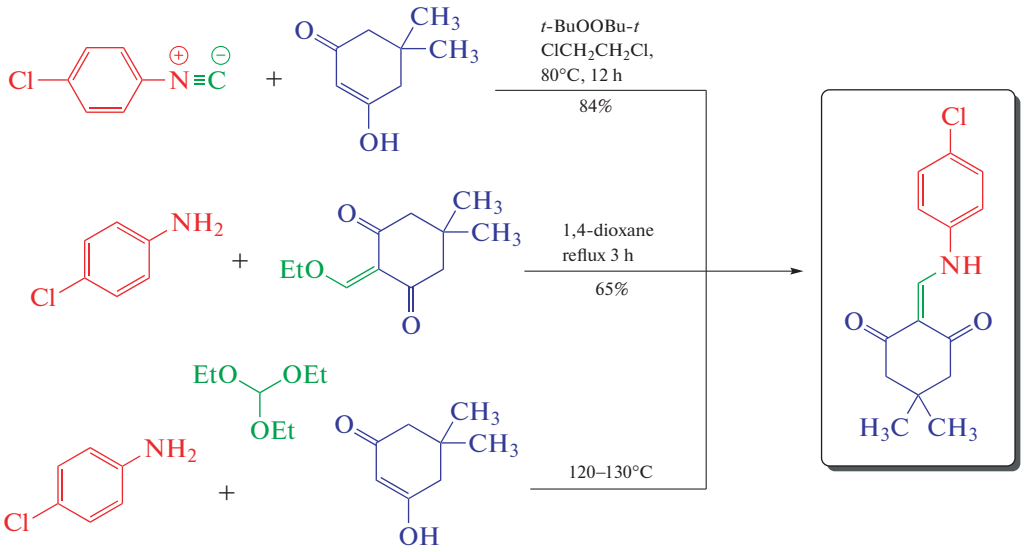

Scheme 1. Possible methods for the synthesis of 2-[((4-chlorophenyl)amino)methylene]-5,5-dimethylcyclohexane-1,3-dione.

This work is devoted to the design, synthesis, and characterization of the coordination compounds of the lanthanide(III) series with 2-[((4-chlorophenyl)amino)methylene]-5,5-dimethylcyclohexane-1,3-dione and to the detailed study of the photoluminescence properties of the synthesized complexes.

EXPERIMENTAL

The following commercial reagents were used as purchased for the synthesis of the coordination compounds: lanthanide(III) nitrates (99.9%, Sigma-Aldrich), propanol-2 (reagent grade), and dichloromethane (reagent grade).

Synthesis of 2-[((4-chlorophenyl)amino)methylene]-5,5-dimethylcyclohexane-1,3-dione (L). A mixture of dimedone (1.00 g, 7.1 mmol), 4-chloroaniline (0.90 g, 7.1 mmol), and freshly distilled triethyl orthoformate (1.5 mL, 9.0 mmol) was heated in a 20-mL vial with vigorous stirring to the complete homogenization of the reaction mixture and beginning of boiling. The crystallization of the reaction mixture was observed in 1–2 min. The mixture was cooled down, and the precipitate was filtered off and recrystallized from *n*-butanol. The crystals as colorless needles were separated, washed with butanol and petroleum ether, and dried at 75°C. The yield after recrystallization was 1.47 g (74%). The purity of the organic ligand was confirmed by NMR spectroscopy (Scheme 2).

^{1}H NMR (500 MHz, $CDCl_3$; δ, ppm): 1.04 (s, 6H, CH_3), 2.37 (s, 2H, 4-CH_2), 2.41 (s, 2H, 6-CH_2), 7.15 (d, 2H, J = 8.8 Hz, 2'-CH), 7.33 (d, 2H, 3'-CH), 8.48 (d, 1H, J = 13.5 Hz, 2-CH), 12.8 (br.d, 1H, NH). ^{13}C NMR (126 MHz, $CDCl_3$; δ, ppm): 28.64 (CH_3), 31.20 (5-C), 51.40 (4-C), 51.76 (6-C), 109.22 (1-C), 119.40 (2'-C), 130.16 (3'-C), 131.88 (4'-C), 137.25 (1'-C), 150.24 (2-C), 196.21 (3-C; $^2J_{CH}$ = 6 Hz, $^3J_{cis\text{-}CH}$ = 3 Hz), 200.19 (7-C; $^2J_{CH}$ = $^3J_{trans\text{-}CH}$ = 6.4 Hz). ^{15}N NMR (51 MHz, $HCONH_2$; δ, ppm): 138.0 ($^1J_{NH}$ = 90 Hz).

IR (ν, cm^{-1}): 3236–3161 ν(NH); 2957, 2924, 2868, 2853 ν(CH_2, CH_3); 1477–1431, 1408, 1377, 1211, 1188–1124, 1030, 974, 831 δ(CH_2, CH_3); 1653, 1616, 1593, 1576 ν(C=O); 1558, 1317–1246, 1188–1124, 1078, 864 R_{ring}.

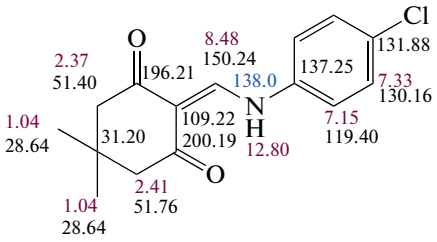

Scheme 2. Structural formula of 2-[((4-chlorophenyl)amino)methylene]-5,5-dimethylcyclohexane-1,3-dione (L) and band assignment of the ligand according to the NMR spectroscopic data.

Synthesis of $[EuL_2(NO_3)_3]_n$ (I). A weighed sample of the ligand (1.0 mmol, 0.27 g) was added with stirring to a solution of $Eu(NO_3)_3 \cdot 6H_2O$ (1.0 mmol, 0.44 g) in isopropyl alcohol (5.0 mL). A white precipitate of the complex was formed within 0.5 h after ligand L was dissolved. The formed precipitate was filtered through a glass filter, washed with isopropyl alcohol, and dried in air. The yield of compound **I** was 0.39 g (87%).

IR (ν, cm^{-1}): 3237–3159 ν(NH); 2957, 2926, 2872–2856 ν(CH_2, CH_3); 1485, 1464, 1454, 1–1537, 1317, 1298, 1271, 1157, 1136, 1124, 862 R_{ring}, 1498, 1337, 816 ν(NO_3^-).

For $C_{30}H_{32}N_5O_{13}Cl_2Eu$

Anal. calcd., %	C, 40.3	H, 3.6	N, 7.8
Found, %	C, 40.0	H, 3.9	N, 7.8

Synthesis of $[SmL_2(NO_3)_3]_n$ (II) was conducted according to a procedure similar to that for compound **I** using samarium(III) nitrate hexahydrate instead of europium(III) nitrate hexahydrate. The molar ratio of the reactants in the synthesis was 1 : 1, and the load was decreased by two times compared to that in the synthesis of complex **I** (0.50 mmol). The formed precipitate was washed with dichloromethane. The yield of compound **II** was 0.17 g (77%).

IR (ν, cm^{-1}): 3238–3167 ν(NH); 2957, 2926, 2878–2856 ν(CH_2, CH_3); 1485, 1466, 1454, 1437, 1412, 1385, 1371, 1217, 1178, 976, 831 δ(CH_2, CH_3); 1661, 1609–1533 ν(C=O); 1609–1533, 1315, 1296, 1271, 1159, 1136, 1124, 860 R_{ring}, 1499, 1338, 816 ν(NO_3^-).

For $C_{30}H_{32}N_5O_{13}Cl_2Sm$

Anal. calcd., %	C, 40.4	H, 3.6	N, 7.8
Found, %	C, 39.6	H, 3.4	N, 7.8

Synthesis of $[TbL_2(NO_3)_3]_n$ (III) was carried out according to a procedure similar to that for compound **I** using terbium(III) nitrate hexahydrate instead of europium(III) nitrate hexahydrate. The mother liquor was left to stay for crystallization at ~4°C, and colorless single crystals were formed in 2 weeks. The yield of compound **III** was 0.15 g (82%).

IR (ν, cm^{-1}): 3240–3179 ν(NH); 2959, 2924, 2870–2845 ν(CH_2, CH_3); 1485, 1466, 1454, 1437, 1412, 1385, 1371, 1217, 1178, 976, 831 δ(CH_2, CH_3); 1663, 1607–1535 ν(C=O); 1607–1535, 1317, 1298, 1271, 1157, 1136, 1124, 862 R_{ring}, 1499, 1338, 814 ν(NO_3^-).

For $C_{30}H_{32}N_5O_{13}Cl_2Tb$

Anal. calcd., %	C, 40.0	H, 3.6	N, 7.8
Found, %	C, 39.9	H, 3.5	N, 7.7

Synthesis of $[DyL_2(NO_3)_3]_n$ (IV). Ligand L (0.5 mmol, 0.14 g) dissolved in dichloromethane (1.0 mL) was added on stirring to an isopropanol solution (3.0 mL) of $Dy(NO_3)_3 \cdot 5H_2O$ (1.0 mmol, 0.44 g). A white precipitate formed after prolong stirring was filtered through a glass filter, washed with isopropyl alcohol, and dried in air. The yield of compound **IV** was 0.14 g (62%).

IR (ν, cm^{-1}): 3252–3173 ν(NH); 2961, 2936, 2883–2860 ν(CH_2, CH_3); 1483, 1464, 1454, 1437, 1410, 1389, 1369, 1217, 1178, 976, 829 δ(CH_2, CH_3); 1663, 1607–1535 ν(C=O); 1607–1535, 1317, 1304, 1271, 1157, 1134, 860 R_{ring}, 1499, 1338, 814 ν(NO_3^-).

For $C_{30}H_{32}N_5O_{13}Cl_2Dy$

Anal. calcd., %	C, 39.9	H, 3.6	N, 7.7
Found, %	C, 39.8	H, 3.4	N, 7.9

Synthesis of $[GdL_2(NO_3)_3]_n$ (V). Ligand L (0.5 mmol, 0.14 g) dissolved in dichloromethane (2.5 mL) was added on stirring to an isopropanol solution (2.0 mL) of $Gd(NO_3)_3 \cdot 6H_2O$ (0.5 mmol, 0.22 g). A white precipitate formed after prolong stirring was filtered through a glass filter, washed with isopropyl alcohol, and dried in air. The yield of compound **V** was 0.17 g (77%).

IR (ν, cm^{-1}): 3237–3159 ν(NH); 2957, 2926, 2872–2856 ν(CH_2, CH_3); 1485, 1464, 1454, 1–1537, 1317, 1298, 1271, 1157, 1136, 1124, 862 R_{ring}, 1498, 1337, 816 ν(NO_3^-).

For $C_{30}H_{32}N_5O_{13}Cl_2Gd$

Anal. calcd., %	C, 40.1	H, 3.6	N, 7.8
Found, %	C, 39.8	H, 3.4	N, 7.9

Elemental (C, H, N) analysis was carried out at the Analytical Laboratory of the Nikolaev Institute of Inorganic Chemistry (Siberian Branch, Russian Academy of Sciences) on a Vario MICRO cube CHNS-analyzer. The IR spectra of the samples prepared as suspensions in Vaseline and in fluorinated oil

Table 1. Crystallographic data and the experimental and structure refinement parameters for compounds L and **III**

Parameter	Value	
	L	**III**
Empirical formula	$C_{15}H_{16}NO_3Cl$	$C_{30}H_{32}N_5O_{13}Cl_2Tb$
FW	277.74	900.42
Temperature, K	288	150
Crystal system	Triclinic	Monoclinic
Space group	$P\bar{1}$	$C2/c$
a, Å	5.7334(3)	14.3756(6)
b, Å	11.0450(7)	11.6235(4)
c, Å	11.3201(6)	20.8054(8)
α, deg	103.111(5)	90
β, deg	98.752(4)	92.691(2)
γ, deg	97.149(5)	90
V, Å^3	680.56(7)	3472.6(2)
Z	2	4
ρ_{calc}, g/cm^3	1.355	1.722
μ, mm^{-1}	0.278	2.262
Crystal size, mm^3	0.12 × 0.06 × 0.05	0.06 × 0.05 × 0.03
Scan range over 2θ, deg	3.76–57.91	4.86–55.01
Range of indices *hkl*	$-7 \le h \le 7$, $-14 \le k \le 11$, $-13 \le l \le 14$	$-18 \le h \le 18$, $-15 \le k \le 15$, $-26 \le l \le 26$
Number of reflections measured/independent	5582/2961	18112/3969
R_{int}, R_{sigma}	0.0211, 0.0397	0.0712, 0.0623
Number of restraints/ parameters	0/174	0/234
Goodness-of-fit for F^2	1.068	1.057
R_1, wR_2 ($I > 2\sigma(I)$)	0.0454, 0.0986	0.0384, 0,0791
R_1, wR_2 (for all reflections)	0.0712, 0.1199	0.0484, 0.0826
Residual electron density (max/min), e Å^{-3}	0.17/–0.23	1.63/–0.74

were recorded on a Scimitar FTS 2000 FT-IR spectrometer in a range of 4000–400 cm^{-1}. Powder XRD analysis was carried out on a Bruker D8 Advance diffractometer (CuK_α radiation, λ = 1.54056 Å, Ni filter, 2θ range from 5° to 40°, acquisition 1 s per point).

NMR spectra were recorded for the ligand (28 mg) dissolved in $CDCl_3$ (0.6 mL) at room temperature on a Bruker Avance III 500 FT-IR spectrometer with working frequencies of 499.93, 125.71, and 50.66 MHz for ^{1}H, ^{13}C, and ^{15}N, respectively.

The diffuse reflectance spectra of the polycrystalline ligand and complex **III** were recorded on a Shimadzu UV-3101PC spectrophotometer in a range of 240–800 nm with a gap width of 5 nm. The calibration accuracy of the wavelength axis was ±0.3 nm for the UV and visible ranges, and measurement inaccuracies related to the scattered light were 0.01%. Barium sulfide served as the standard. Diffuse reflectance spectra were recorded to calculate the absorbance in relative units using the classical Kubelka–Munk function.

Single crystal XRD analysis of ligand L was carried out on an Agilent Xcalibur diffractometer with an AtlasS2 detector at 288 K, and for complex **III**—on a Bruker D8 Venture diffractometer at 150 K. Monochromatic graphite MoK_α radiation (λ = 0.71073 Å) was used. Absorption corrections were applied using the CrysAlisPro [50] (for Agilent Xcalibur) and SADABS [51] (for Bruker D8 Venture) programs. The structures were solved and refined using the SHELXT [52] and SHELXL [53] software in the OLEX2 graphical interface [54]. Atomic thermal displacement parameters for non-hydrogen atoms were refined anisotropically. Positions of hydrogen atoms were calculated geometrically and refined by the riding model. The crystallographic data and information on the refined structures are given in Table 1.

The full crystallographic information was deposited with the Cambridge Crystallographic Data Centre (CIF files CCDC nos. 2298715 (L) and 2298716 (**III**); http://www.ccdc.cam.ac.uk/data_request/cif).

The photoluminescence properties were studied at room temperature for polycrystalline samples on an FLSP920 spectrofluorimeter (Edinburg Instruments) equipped with a xenon lamp and an EPL-375 diode laser. A xenon lamp was used for recording emission and luminescence excitation spectra, and an EPL-375 diode laser (Edinburg Instruments, λ_{exc} = 375 nm, pulse duration 70 ps) served as the excitation source to detect the fluorescence kinetics of the ligand. Absolute quantum yields were measured using the Quanta-φ integrating sphere on a Fluorolog 3 spectrometer (Horiba Jobin Yvon) with a PC177CE-010 cooled module of photon registration and an R2658 photomultiplier. A Fluorolog 3 instrument was used to detect the phosphorescence kinetics of the lanthanide(III) complexes as well as phosphorescence of gadolinium(III) compound with a pulse delay of 0.15 ms (λ_{exc} = 390 nm, 77 K).

RESULTS AND DISCUSSION

Organic ligand L was synthesized according to a modified Wolfbeis procedure [38, 39]: 4-chloroaniline and triethyl orthoformate were added to dimedone followed by the reflux of the prepared solution with stirring. The REE coordination compounds based on L were synthesized in isopropyl alcohol at a molar ratio of 1 : 1 or 2 : 1. A weighed sample of the ligand was added to lanthanide(III) nitrate dissolved in isopropanol. According to this procedure, complexes **I**–**III** were isolated as white precipitates. The addition of the ligand dissolved in dichloromethane to lanthanide(III) nitrate also results in the formation of a white precipitate with the composition similar to that isolated in the synthesis of the dysprosium(III) (**IV**) and gadolinium (**V**) complexes (Scheme 3). According to the elemental analysis data, the coordination compounds with the general formula $[LnL_2(NO_3)_3]$ are formed, and complexes **I**–**V** are isomorphic according to the powder XRD analysis results (Fig. 1).

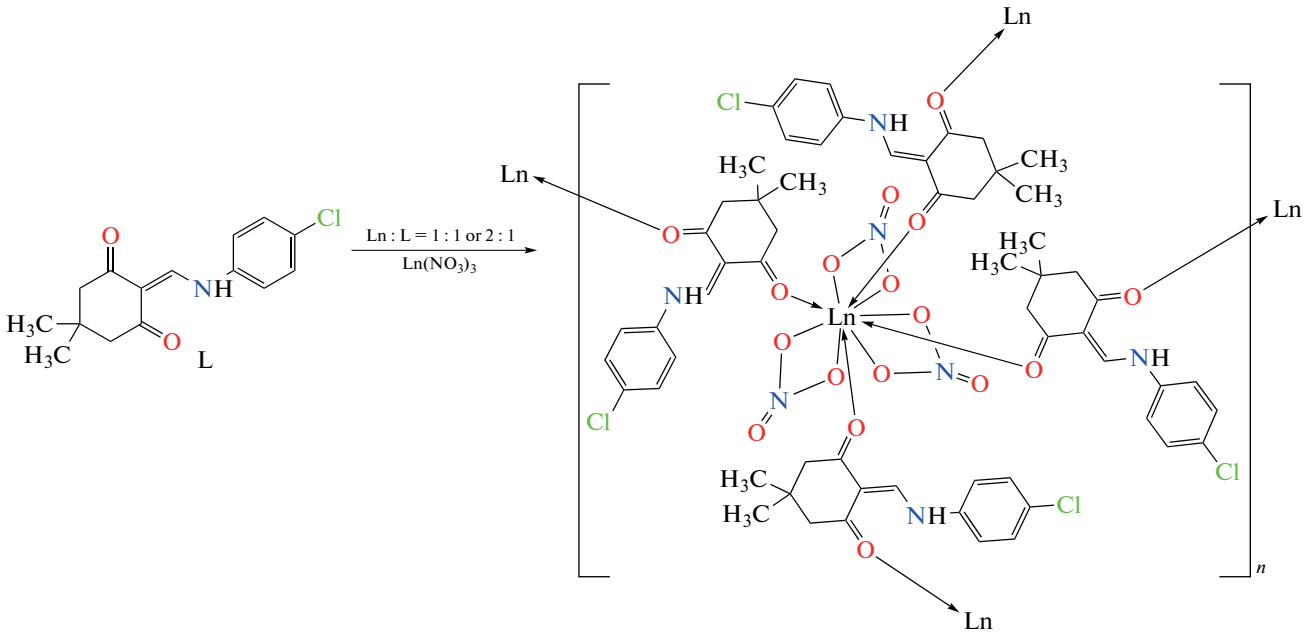

Scheme 3. Scheme for the synthesis of complexes **I**–**V**.

No ligand deprotonation occurs during complex formation, and the NH bond vibrations appear in the IR spectra of the ligand and complexes as a broad band in a range of 3240–3150 cm^{-1}. The intensity of the vibration band of the C=O bond at ~1661 cm^{-1} increases in the spectra of the complexes, and the bands at 1616, 1593, and 1576 cm^{-1} observed in the spectrum of the ligand for the C=O bond appear as a broadened band in the spectra of the complexes. These changes for the carbonyl bond vibrations indicate that this group is involved in coordination to the metal ions. The C–H group stretching vibrations appear in a range of 2960–2850 cm^{-1}, the bending vibrations are observed at 1480–830 cm^{-1}, and the stretching–bending vibrations of the phenyl group are observed at 1560–860 cm^{-1}.

According to the XRD data, L crystallizes in the centrosymmetric space group $P\bar{1}$ (triclinic crystal system). The intramolecular hydrogen bond N–H···O

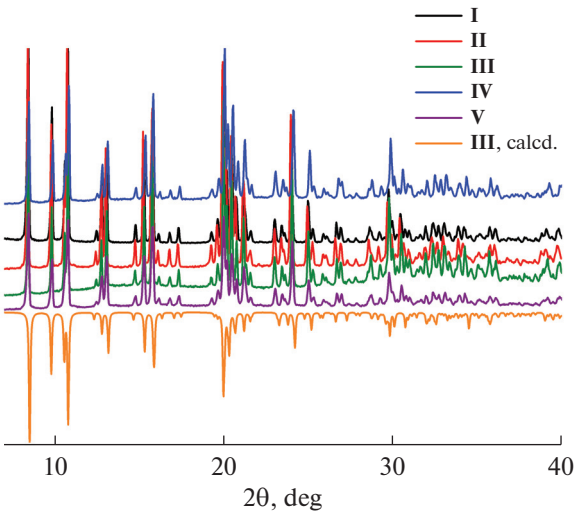

Fig. 1. Powder diffraction pattern calculated from the single-crystal structure (orange line) and experimental powder XRD patterns of the $[LnL_2(NO_3)_3]_n$ complexes.

with a distance between the hydrogen and oxygen atoms of 1.96 Å is observed and retained upon complex formation. The benzene and cyclohexane rings are arranged in one plane, and the C(H)–C–N–C(H) torsion angle (φ_t) passing through two carbon atoms of the phenyl group and the nitrogen and carbon atoms of the enaminone fragment is 4.04° (Fig. 2). The presence of the chlorine atom in the system leads to the formation of noncovalent Cl···Cl interactions between the adjacent molecules with a distance between the atoms of 3.42 Å.

Among the whole series of the lanthanide(III) complexes, single crystals suitable for XRD were obtained only for the terbium(III) compound. The complex crystallizes in the *C*2/*c* space group with the monoclinic crystal system. The coordination sphere of the terbium(III) ion consists of ten oxygen atoms (Fig. 3). The oxygen atoms of the cyclohexanedione fragment are involved in the coordination to the central atom, and the ligand demonstrates the bidentate-bridging coordination mode. This coordination results in the formation of a polymeric layered structure parallel to the *ab* crystallographic plane (Fig. 3). According to the SHAPE analysis data, the coordination polyhedron is close to a two-capped square antiprism with the parameter $S(D4d) = 2.73$. As mentioned above, the phenyl group and enaminone fragment of the uncoordinated ligand lie in one plane, a significant turn of the phenyl group is observed upon complex formation, and the torsion angle increases to 33.07°.

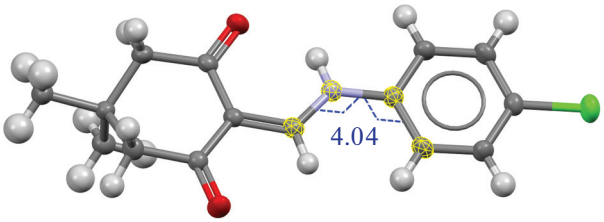

Fig. 2. Structure of the ligand and C(H)–C–N–C(H) torsion angle (φ_t) in L.

The Tb–O(L) bond lengths are 2.44 and 2.34 Å, and the Tb–O(NO_3) bond lengths range from 2.46 to 2.58 Å.

Complex **III** is isostructural to the earlier presented lanthanide(III) complexes with 2-[((4-methoxy)-amino)methylene]-5,5-dimethylcyclohexane-1,3-dione (L') [32]. The polymeric compounds of the identical composition $[Ln(L')_2(NO_3)_3]_n$ also crystallize in the monoclinic crystal system with the space group *C*2/*c*, and the torsion angles of the ligand increase upon complex formation and range from 27.4° to 28.4°. The Ln–O bond lengths are well consistent with those of two series of the compounds, which is distinctly seen when the structures are superimposed (Fig. 4).

Ligand L emits in the blue visible range as a broadened band (Fig. 5). The luminescence quantum yield of L is 22% at $\lambda_{exc} = 370$ nm. The kinetic curve of photoluminescence decay is described by a biexponential function, and the lifetimes of the excited state are 0.6 (52%) and 1.7 ns (48%) (Fig. 6). The presence and position of the substituent in the benzene ring affect the photoluminescence parameters of the organic compounds, which is confirmed by the works dealing with 2-[(phenylamino)methylene]-5,5-dimethylcyclohexane-1,3-dione [30], 2-[((4-methoxy)amino)methylene]-5,5-dimethylcyclohexane-1,3-dione [32], and 2-[((3-methoxy)-amino)-methylene]-5,5-dimethylcyclohexane-1,3-dione [31]. For instance, the quantum yields and lifetimes of the excited states are considerably higher for the compounds with the substituents in the para position of the benzene ring compared to the unsubstituted β-enaminedione derivative. On the contrary, both the emission intensity and quantum yield decrease significantly for the ligand with the methoxy group in the meta position of the benzene ring. Thus, the quantum yield increases in the following order (only substituents and their positions in the benzene ring are designated for brevity):

meta-OCH_3 < unsubstituted < *para*-Cl(L) < *para*-OCH_3.

The luminescence excitation spectra during complex formation are analogous to the spectrum of the ligand and are well consistent with the diffuse reflectance spectra (Fig. 5). The emission spectrum of the

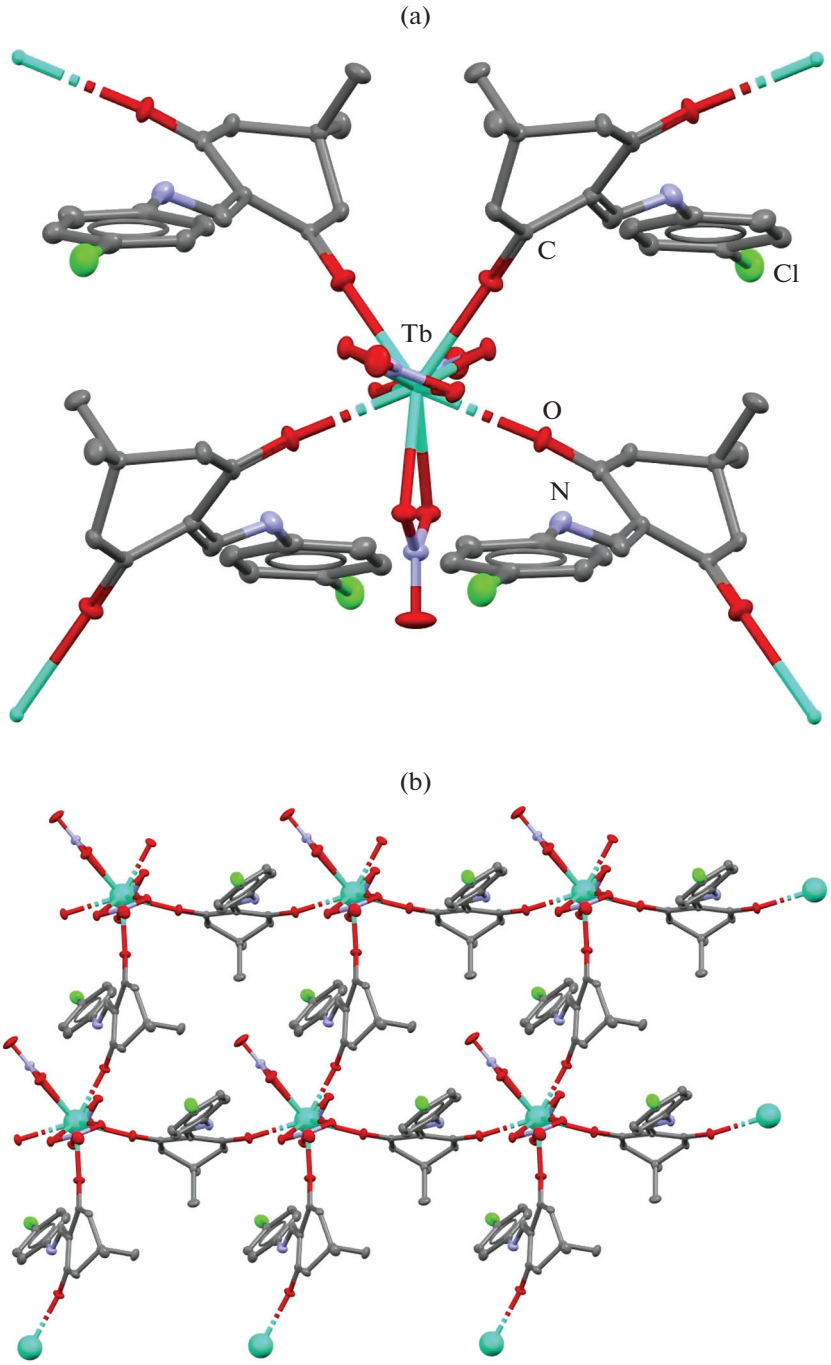

Fig. 3. (a) Coordination node of the $[TbL_2(NO_3)_3]_n$ complex (**III**) and (b) the polymeric layered structure. Hydrogen atoms are omitted.

europium(III) complex (**I**) exhibits only narrow bands of the $^5D_0 \rightarrow {}^7F_J$ transitions ($J = 1$, 2, and 4), unlike the emission spectra of the samarium(III) (**II**) and terbium(III) (**III**) complexes. The spectrum of compound **II** exhibits a low-intensity fluorescence band of the ligand and narrow bands corresponding to the $^4G_{5/2} \rightarrow {}^6H_J$ transitions ($J = 5/2–11/2$). The emission spectrum of complex **III** is a good agreenment with the spectrum of the ligand but has additional bands with a low intensity assigned to the $^5D_4 \rightarrow {}^7F_J$ transitions, where $J = 6–3$ (Fig. 5). The quantum yield of the europium(III) complex is 21.9% ($\lambda_{exc} = 375$ nm),

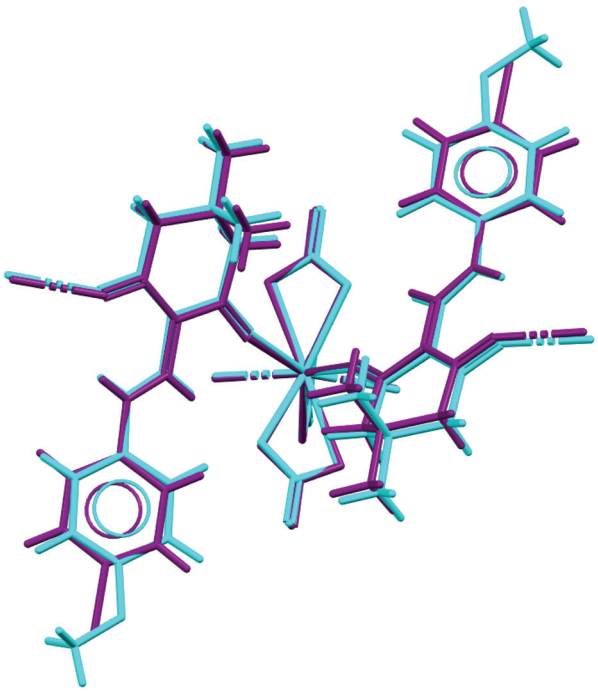

Fig. 4. Superposition of the crystal structures of complexes $[TbL_2(NO_3)_3]_n$ (**III**, violet) and $[Tb(L')_2(NO_3)_3]_n$ (Cambridge Structural Database, turquoise).

and that of the samarium(III) complex is lower than 1%. The lifetime of the excited state of compound **I** is 1.17 ms, and that for complex **II** is 0.034 ms (Fig. 6).

The emission spectrum of the dysprosium(III) complex (**IV**) resembles the luminescence spectrum of the ligand. Phosphorescence investigation of the gadolinium(III) complex (**V**) at 77 K and the decomposition of the obtained spectrum into the Gaussian functions showed that the triplet level energy of the ligand was 20325 cm^{-1} (Fig. 7). Thus, the "antenna" mechanism for the dysprosium(III) complex is not observed, since the radiative level of the Dy(III) ion is higher than the triplet level of the ligand.

The transformation of the recorded emission spectra into the chromaticity coordinates (CIE) makes it possible to see the final emission color of the ligand and complexes (Fig. 8). In addition, the purity of the emission color (saturation) can be determined using the color coordinates. This parameter demonstrates how close is the studied color to the monochromatic color and is calculated by the equation

$$\text{Color purity} = \frac{\sqrt{(x-x_w)^2+(y-y_w)^2}}{\sqrt{(x_d-x_w)^2+(y_d-y_w)^2}}\times 100\%,$$

where x and y are the CIE coordinates of the initial spectrum, x_w and y_w are the CIE coordinates of the white color, and x_d and y_d are the CIE coordinates of the dominating wavelength (red, green, or blue). The dominating wavelength of the ligand was chosen to be 450 nm (blue color), and 615 nm (red color) was chosen for the europium(III) and samarium(III) complexes. This parameter for the ligand reaches 84.79%, and those for compounds **I** and **II** are 92.01 and

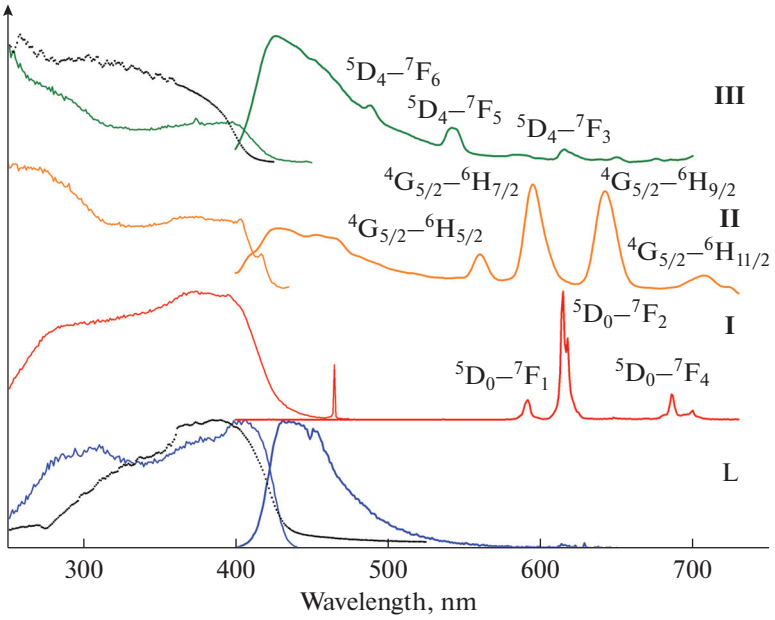

Fig. 5. Diffuse reflectance spectra (dashed lines) and the luminescence excitation and emission spectra for the ligand and complexes **I**–**III**. The emission spectra were detected at λ_{exc} = 370 nm, and the luminescence excitation spectra were recorded at λ_{em} = 460 nm for L, λ_{em} = 613 nm for the europium(III) complex, λ_{em} = 594 nm for the samarium(III) complex, and λ_{em} = 545 nm for the terbium(III) complex.

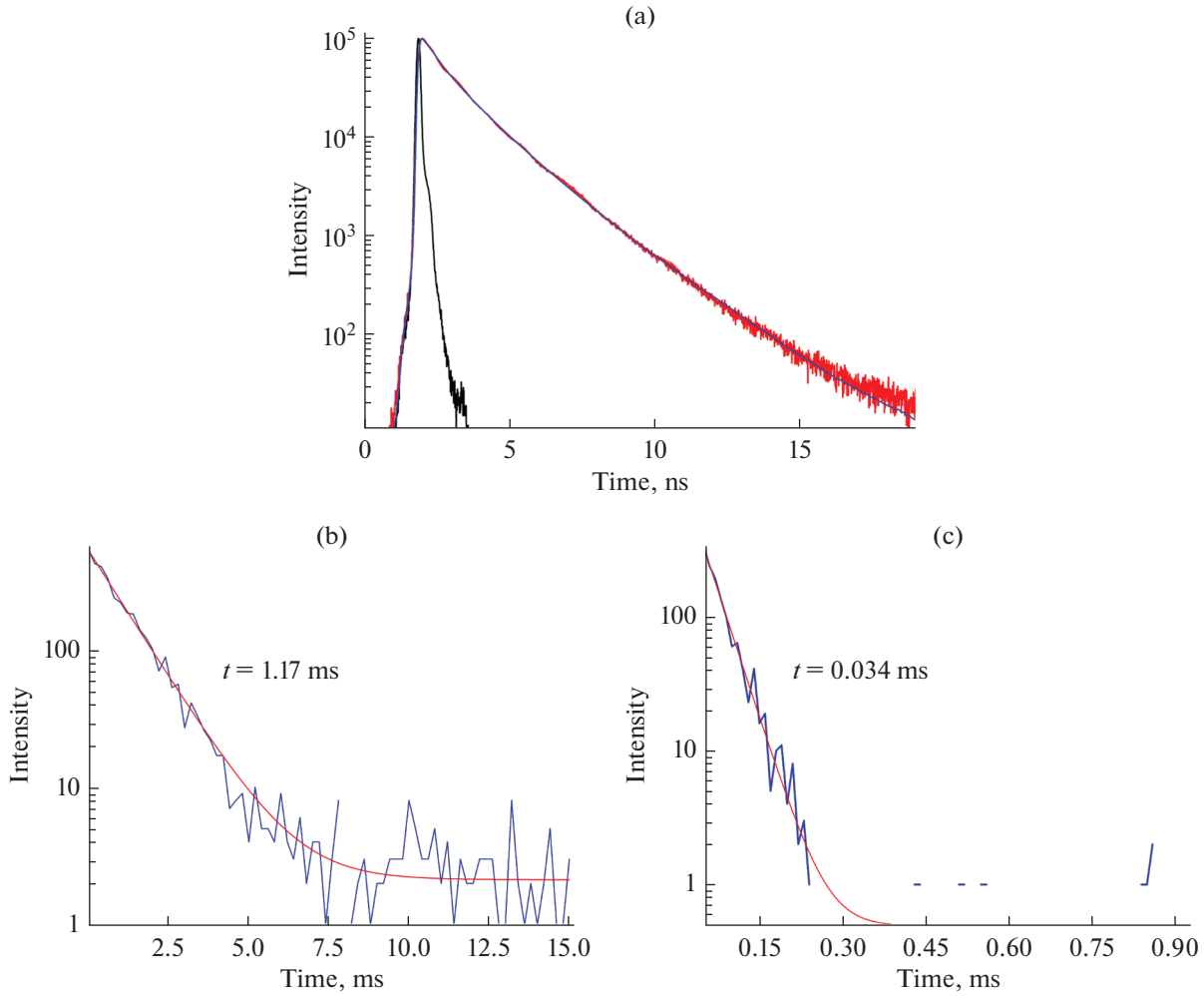

Fig. 6. Luminescence kinetic curves of the ligand and complexes: (a) the kinetic curve of L is designated by red at λ_{exc} = 375 nm and λ_{em} = 470 nm, the biexponential approximation is shown by blue with lifetimes of 0.6 ns (52%) and 1.7 ns (48%), and the instrumental response function is black; (b) the kinetic curve of the europium(III) complex is designated by blue at λ_{exc} = 370 nm and λ_{em} = 615 nm and the approximation is red with a characteristic time of 1.17 ms; and (c) the kinetic curve of the samarium(III) complex is designated by blue at λ_{exc} = 370 nm and λ_{em} = 595 nm and the approximation is red with a characteristic time of 0.034 ms.

18.68%, respectively. Thus, the CIE chromaticity and color purity coordinates are necessary to characterize the color stimulus, and the color purity of the main color emissions should be higher than 90% according to the GOST R 52870-2007 ("Facilities of Collective Use for Information Imaging. Requirements on Visual Information Imaging and Measurement Methods").

The percentage of absorbed photons leading to the energy transfer to the REE ion are reflected as the parameter of sensitization efficiency (η), which is defined as the ratio of the total quantum yield (φ_L^{Ln}) to the internal quantum yield $\left(\varphi_{Ln}^{Ln}\right)$. The φ_L^{Ln} parameter can directly be measured when studying the photoluminescence properties of the compounds, and φ_{Ln}^{Ln} is calculated from the measured lifetime of the excited

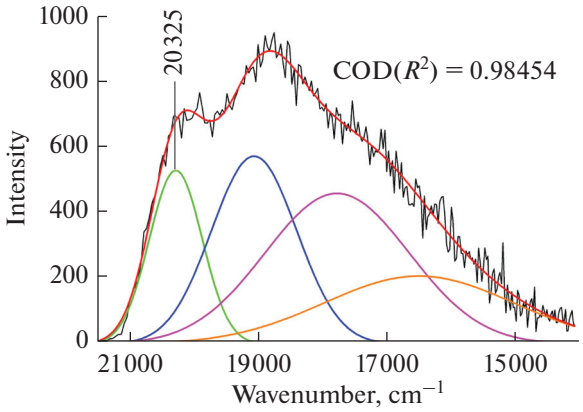

Fig. 7. Phosphorescence spectrum of complex **V** at 77 K and the decomposition of the spectrum into the Gaussian functions.

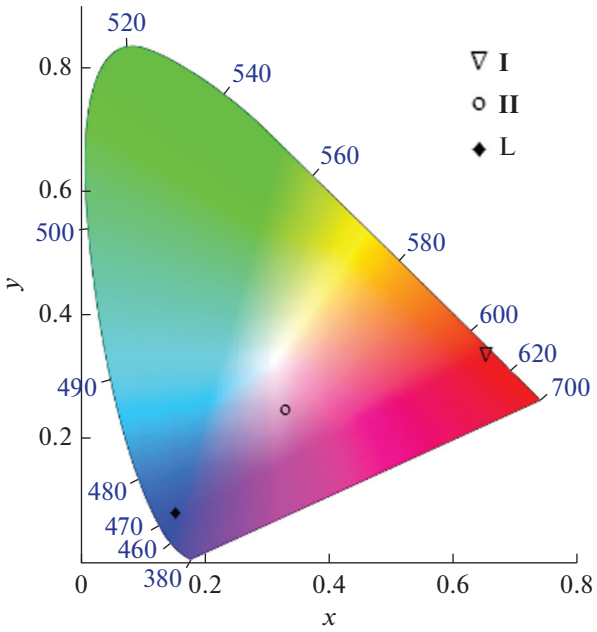

Fig. 8. Color space CIE1931 reflecting the emission color of the ligand and complexes **I** and **II**.

state (τ_{obs}) and radiative lifetime (τ_{rad}): $\varphi_{Ln}^{Ln} = \frac{\tau_{obs}}{\tau_{rad}}$. In the case of the europium(III) ion, the calculation of τ_{rad} is reduced to rather simple equation, since this ion is characterized by the magnetic dipole transition $^5D_0 \rightarrow {}^7F_1$, whose intensity is nearly independent of the coordination environment. As a result, the integral values of the total emission spectrum (I_{tot}) and transition band $^5D_0 \rightarrow {}^7F_1$ (I_{MD}) are needed for the calculation of τ_{rad}

$$\frac{1}{\tau_{rad}} = A_{MD,0} n^3 \frac{I_{tot}}{I_{MD}},$$

where parameter $A_{MD,0}$ reflects the probability of spontaneous emission for $^5D_0 \rightarrow {}^7F_1$ in vacuum, and n is the refractive index of the medium. According to the published data, $A_{MD,0}$ corresponds to 14.65 s^{-1} [55–59]. Using measured τ_{obs} and φ_L^{Ln} for complex **I** it is found $\varphi_{Ln}^{Ln} = 50\%$ and $\eta = 43.5\%$. The sensitization efficiency for compound **I** is highest among the earlier presented europium(III) complexes [30–32].

Thus, five polymeric lanthanide(III) complexes based on 2-[((4-chlorophenyl)amino)methylene]-5,5-dimethylcyclohexane-1,3-dione with the general formula $[LnL_2(NO_3)_3]_n$ were synthesized. The structures of the new compounds were determined by XRD analysis for single crystals of terbium(III) complex **III**. The organic ligand exhibits the bidentate-bridging coordination resulting in the formation of the polymeric layered compounds, and the nitrate ions is coordinated via the chelating mode. As confirmed by the powder XRD analysis data, the synthesized polycrystalline compounds and single crystals of complex **III** are isostructural. The organic ligand demonstrates fluorescence in the blue range of electromagnetic radiation with nanosecond lifetimes of the excited states. The energy transfer from the ligand to lanthanide(III) ion during complex formation occurs for the europium(III) (**I**), samarium(III) (**II**), and terbium(III) (**III**) compounds. The maximum quantum yield is observed for complex **I** (21.9%), and the sensitization efficiency is 43.5%.

ACKNOWLEDGMENTS

The authors are grateful to A.P. Zubareva and N.N. Komardina for elemental analysis data, V.N. Yudin for presented data measured at the Center for Collective Use of the Nikolaev Institute of Inorganic Chemistry (Siberian Branch, Russian Academy of Sciences), M.O. Matveeva for conducting powder XRD analysis, A.A. Sh-povalova for recording IR spectra, A.A. Ryadun for detecting quantum yields and long lifetimes of excited states, and A.S. Berezin for recording the phosphorescence spectrum. The authors are grateful to the Ministry of Science and Higher Education of the Russian Federation (projects nos. 121031700321-3 and FWGF-2021-0005).

FUNDING

This work was funded by Russian Science Foundation (the agreement no. 23-23-10028 of April 20, 2023) and the government of the Novosibirsk region of the Russian Federation (agreement no. r-65 of April 3, 2023), project no. 23-23-10028.

CONFLICT OF INTEREST

The authors of this work declare that they have no conflicts of interest.

REFERENCES

1. Bünzli, J.C.G., *Chem. Rev.*, 2010, vol. 110, no. 5, p. 2729.
2. Aspinall, H.C., *Chem. Rev.*, 2002, vol. 102, no. 6, p. 1807.
3. Hasegawa, Y., Kitagawa, Y., and Nakanishi, T., *NPG Asia Mater.*, 2018, vol. 10, no. 4, p. 52.
4. Bao, G., Wen, S., Lin, G., et al., *Coord. Chem. Rev.*, 2021, vol. 429, p. 213642.
5. Wei, C., Ma, L., Wei, H.B., et al., *Sci. China Technol. Sci.*, 2018, vol. 61, no. 9, p. 1265.
6. Armelao, L. and Quici, S., *Coord. Chem. Rev.*, 2010, vol. 254, nos. 5–6, p. 48705.
7. Bryleva, Y.A., Komarov, V.Y., Glinskaya, L.A., et al., *New J. Chem.*, 2023, vol. 47, no. 21, p. 10446.
8. Bryleva, Y.A., Artem'ev, A.V., Glinskaya, L.A., et al., *J. Struct. Chem.*, 2021, vol. 62, no. 2, p. 265.
9. Bryleva, Y.A., Artem'ev, A.V., Glinskaya, L.A., et al., *Inorg. Chim. Acta*, 2021, vol. 516, p. 120097.
10. Artem'ev, A.V., Gusarova, N.K., Malysheva, S.F., et al., *Mendeleev Commun.*, 2012, vol. 22, no. 6, p. 294.
11. Crosby, G.A., Whan, R.E., and Freeman, J.J., *J. Phys. Chem.*, 1962, vol. 6, no. 12, p. 2493.
12. Rao, V.S. and Sauve, G., *Comprehensive Organic Functional Group Transformations*, 1995, vol. 2, p. 737.
13. Chiara, J.L., *Comprehensive Organic Functional Group Transformations II*, 2005, p. 709.
14. Lue, P. and Greenhill, J.V., *Adv. Heterocycl. Chem.*, 1996, vol. 67, p. 207.
15. Aly, A.A. and Hassan, A.A., *Adv. Heterocycl. Chem.*, 2014, vol. 112, p. 145.
16. Ebenezer, W.J. and Wight, P., *ChemInform*, 1996, p. 20576.
17. Liu, T., Wan, J.P., and Liu, Y., *Chem. Commun.*, 2021, vol. 57, no. 72, p. 9112.
18. Yu, T., Ji, F., Huang, D., et al., *Org. Chem. Front.*, 2021, vol. 8, no. 20, p. 5716.
19. Wan, J.P., Cao, S., and Liu, Y., *Org. Lett.*, 2016, vol. 18, no. 23, p. 6034.
20. Stanovnik, B., *Eur. J. Org. Chem.*, 2019, vol. 2019, nos. 31–32, p. 5120.
21. Gao, Y., Liu, Y., and Wan, J.P., *Org. Chem.*, 2019, vol. 84, no. 4, p. 2243.
22. Edafiogho, I.O. and Kombian, S.B., *J. Pharm. Sci.*, 2007, vol. 96, no. 10, p. 2509.
23. Bimoussa, A., Oubella, A., Hachim, M.E., et al., *J. Mol. Struct.*, 2021, vol. 1241, p. 130622.
24. Masaret, G.S., *ChemistrySelect*, 2021, vol. 6, no. 5, p. 974.
25. Eddington, N.D., Cox, D.S., Khurana, M., et al., *Eur. J. Med. Chem.*, 2003, vol. 38, no. 1, p. 49.
26. Anderson, A.J., Nicholson, J.M., Bakare, O., et al., *Bioorg. Med. Chem.*, 2006, vol. 14, no. 4, p. 997.
27. Amaye, I.J., Harper, T.L., and Jackson-Ayotunde, P., *J. Fluorine Chem.*, 2021, vol. 251, p. 109886.
28. Li, H., Shu, H., Wang, X., et al., *Org. Mater.*, 2020, vol. 02, no. 1, p. 033.
29. Li, H., Shu, H., Liu, Y., et al., *Adv. Opt. Mater.*, 2019, vol. 7, no. 8, p. 1801719.
30. Smirnova, K.S., Ivanova, E.A., Sukhikh, T.S., et al., *Inorg. Chim. Acta*, 2021, vol. 525, p. 120490.
31. Smirnova, K.S., Ivanova, E.A., Eltsov, I.V., et al., *Polyhedron*, 2022, vol. 227, p. 116122.
32. Smirnova, K.S., Ivanova, E.A., Pozdnyakov, I.P., et al., *Inorganica Chim. Acta*, 2022, vol. 542, p. 121107.
33. Jiang, H., Li, Y., Sun, M., et al., *Arkivoc. Arkat.*, 2020, vol. 2020, no. 6, p. 1.
34. Mohareb, R.M., Manhi, F.M., Mahmoud, M.A.A., et al., *Med. Chem. Res.*, 2020, vol. 29, no. 8, p. 1536.
35. Van Tinh, D., Fischer, M., and Stadlbauer, W., *J. Heterocycl. Chem.*, 1996, vol. 33, no. 3, p. 905.
36. Rather, M.A., Lone, A.M., Teli, B., et al., *Medchemcomm*, 2017, vol. 8, no. 11, p. 2133.
37. Wang, J.M., Asami, T., Che, F.S., et al., *J. Agric. Food Chem.*, 1997, vol. 45, no. 7, p. 2728.
38. Wolfbeis, O.S. and Erich Ziegler, E.Z., *Z. Naturforsch., A: Phys. Sci.*, 1976, vol. 31, no. 11, p. 1519.
39. Zacharias, G., Wolfbeis, O.S., and Junek, H., *Monatsh. Chem.*, 1974, vol. 105, no. 6, p. 1283.
40. Fossa, P., Menozzi, G., Dorigo, P., et al., *Bioorg. Med. Chem.*, 2003, vol. 11, no. 22, p. 4749.
41. Frolov, K.A., Dotsenko, V.V., and Krivokolysko, S.G., *Chem. Heterocycl. Compd.*, 2013, vol. 49, no. 9, p. 1301.
42. Komkov, A.V., Prezent, M.A., Ignatenko, A.V., et al., *Russ. Chem. Bull.*, 2006, vol. 55, no. 11, p. 2085.
43. Dotsenko, V.V., Krivokolysko, S.G., Chernega, A.N., et al., *Russ. Chem. Bull.*, 2002, vol. 51, no. 8, p. 1556.
44. Dotsenko, V.V. and Krivokolysko, S.G., *Chem. Heterocycl. Compd.*, 2013, vol. 48, no. 10, p. 1568.
45. Dotsenko, V.V., Frolov, K.A., Krivokolysko, S.G., et al., *Chem. Heterocycl. Compd.*, 2013, vol. 49, no. 3, p. 440.
46. Grannik, V.G., Shanazarov, A.K., Solov'eva, N.P., et al., *Chem. Heterocycl. Compd.*, 1987, vol. 23, no. 11, p. 1171.
47. Qin, J.H. and Han, X.D., *Z. Krist. New Cryst. Struct.*, 2012, vol. 227, no. 1, p. 7.
48. Eremina, Y.A., Ermakova, E.A., Sukhikh, T.S., et al., *J. Struct. Chem.*, 2021, vol. 62, no. 2, p. 309.
49. Yang, L.W., Liu, S., Rettig, S.J., et al., *Inorg. Chem.*, 1995, vol. 34, no. 19, p. 4921.
50. *CrysAlisPro 1.171.38.46*, The Woodlands: Rigaku Oxford Diffraction, 2015.
51. *APEX2 (version 2.0), SAINT (version 8.18c) and SADABS (version 2.11)*, Madison: Bruker Advanced X-ray Solutions, 2000–2012.
52. Sheldrick, G.M., *Acta Crystallogr., Sect. A: Found. Adv.*, 2015, vol. 71, p. 3.
53. Sheldrick, G.M., *Acta Crystallogr, Sect. C: Struct. Chem.*, 2015, vol. 71, p. 3.
54. Dolomanov, O.V., Bourhis, L.J., Gildea, R.J., et al., *J. Appl. Crystallogr.*, 2009, vol. 42, no. 2, p. 339.

55. Werts, M.H.V., Jukes, R.T.F., and Verhoeven, J.W., *Phys. Chem. Chem. Phys.*, 2002, vol. 4, no. 9, p. 1542.
56. Werts, M.H.V., *Luminescent Lanthanide Complexes: Visible Light Sensitised Red and Near-Infrared Luminescence*, Univ. of Amsterdam, 2000.
57. Andres, J. and Chauvin, A.-S., *Encycl. Inorg. Bioinorg. Chem.*, 2012, p. 1.
58. Klink, S.I., Hebbink, G.A., Grave, L., et al., *J. Phys. Chem. A*, 2002, vol. 106, no. 15, p. 3681.
59. Bünzli, J.-C.G. and Eliseeva, S.V., *Lanthanide Luminescence*, Hänninen, P. and Härmä, H., Eds., 2010, vol. 7, p. 1.

Translated by E. Yablonskaya